

In conclusion, the present work shows that different site spectra may appear in $\text{CaF}_2:\text{Gd}^{3+}$ crystals, which have been grown in different ways. The effect of heat treatment was also demonstrated. These results seem to rule out generalizations such as those made by Kiss and Staebler,⁴ according to which in all CaF_2 doped with rare earths, the thermoluminescence is due to rare earth in cubic sites only. On the other hand, our results seem to be parallel to those of Makovsky,⁵ who studied the fluorescence of this material. As for the general glow curve, the various glow peaks do not seem to appear at identical temperatures in different crystals. Nevertheless, one is tempted to assume that the trapping sites are characteristic of the host lattice, as is the case in

the alkali halides.¹³ Since our proposed mechanism for the thermoluminescence would assume these sites to be in close proximity to the rare earth, it is not unexpected then that these sites are influenced by the different symmetries surrounding the rare earths, thus causing changes in activation energies from crystal to crystal.

Finally, it is intended to extend the present work to CaF_2 doped with other rare earths.

ACKNOWLEDGMENT

We wish to thank Dr. H. I. S. Ferguson for the loan of optical equipment used in this investigation.

¹³ M. Schlesinger and A. Halperin, *Phys. Rev. Letters* **11**, 360 (1963).

Positron Annihilation in Real Metals. II. Calculation of Core Enhancement Factors*

J. P. CARBOTTE AND A. SALVADORI

Department of Physics, McMaster University, Hamilton, Ontario, Canada

(Received 10 March 1967)

A first-principle calculation of core-annihilation enhancement factors in sodium and aluminum is presented. The computations are based on a previously developed theory whose numerical results had formerly been only crudely estimated. The core electrons are treated in the tight-binding approximation using atomic wave functions appropriate to the metallic state. The conduction-band states are taken to be single orthogonalized plane waves. The central core-conduction matrix element of the theory is evaluated with one computational approximation: a simplifying angular average. The enhancement factors obtained have a weak momentum dependence, so the shape of the core contribution calculated without correlations is unaffected. The enhanced contribution of the orthogonalization parts of *conduction*-electron wave functions remains to be evaluated, so that comparison of our results with experiment is not completely unambiguous. With this reservation, however, the agreement on the whole is satisfactory for both distributions and total lifetimes.

I. INTRODUCTION

IN a previous paper¹ a theory of positron annihilation was derived, which included band-structure effects while accounting partially for correlation effects between the annihilating electron-positron pair. The work was based on a summation of a select infinite subset of Feynman graphs in the perturbation expansion of the electron-positron Green's function. It is a space-time contraction of this two-body Green's function which determines the annihilation rate in a nonrelativistic system of electrons and positrons. The graphs summed were the ladder diagrams; this approximation was originally introduced, with considerable success, by Kahana² in a discussion of lifetimes in an electron gas. Since then it has been analyzed more critically by Carbotte and Kahana³ and refined by Bergersen⁴ and

by Carbotte.⁵ These refinements of electron-gas theory will not concern us directly here (we will return to them briefly in the last section). They represent only secondary corrections to the main ladder contribution. Also, electron-gas results cannot be taken over directly to the case of core electrons. More important, the ladder graphs have not, as yet, been properly evaluated for core electrons although from the crude estimate supplied in Ref. 1 they are known to give important corrections to the independent-particle model (I.P.M.) extensively used in past discussions of this problem.⁶⁻⁸ The purpose of this paper is to carry out a computation of ladder corrections.

It is not difficult to understand, at least in a general way, the relevance of the ladder approximation to the calculation of lifetimes. The first point to realize is that for an arbitrary system of low-energy electrons and

* Research supported by the National Research Council of Canada.

¹ J. P. Carbotte, *Phys. Rev.* **144**, 309 (1966).

² S. Kahana, *Phys. Rev.* **129**, 1622 (1963).

³ J. P. Carbotte and S. Kahana, *Phys. Rev.* **139**, A213 (1965).

⁴ B. Bergersen, Ph.D., Brandeis University, 1964 (unpublished).

⁵ J. P. Carbotte, *Phys. Rev.* (to be published).

⁶ S. Berko and J. S. Plaskett, *Phys. Rev.* **112**, 1877 (1958).

⁷ E. Daniel, *J. Phys. Chem. Solids* **6**, 205 (1958).

⁸ P. R. Wallace, in *Solid State Physics*, edited by F. Seitz and D. Turnbull (Academic Press Inc., New York, 1960), Vol. 10.

positrons, the annihilation rate is directly proportional to the electronic density at the positron site. This quantity must clearly depend strongly on the short-range correlations between the annihilating pair. Thus, it would seem essential to include, in any given approximate calculation, at least all the multiple scatterings of the electron-positron pair off each other, i.e., sum the particle-particle ladders. The zeroth-order term in this series gives the I.P.M. The remainder represent corrections. We should, perhaps, be more explicit.

In the I.P.M. the positron is taken to propagate through the medium influenced only by the average Hartree field of the electron-plus-ion system. The contribution to the annihilation rate of a given tight-binding-core electron is then given by the overlap of its wave function with the positron Bloch state. This procedure, while simple, ignores much of the important correlations, and accounts for the direct Coulomb force between the positron and annihilating electron only in an average and trivial way. This attractive force certainly influences significantly the relative motion of the pair in their center-of-mass system and must lead to a significant increase of the electronic density at the positron over that computed on the I.P.M. The factor characterizing this increase in electronic density is called the enhancement factor for the pair. For the conduction band these factors can be quite large, of order 10 in sodium. Although, in this case, they depend somewhat on the total center-of-mass momentum of the pair, they are mainly a measure of the coherence in their relative motion.

It is not necessary to stress here that the rather large enhancement factors derived for the conduction electrons are due in part to their free-electron nature. That is, they easily readjust to the positron presence. On the other hand, core electrons are not so free. Their motion is dominated by the screened nuclear field of their respective ion so that the positron Coulomb field

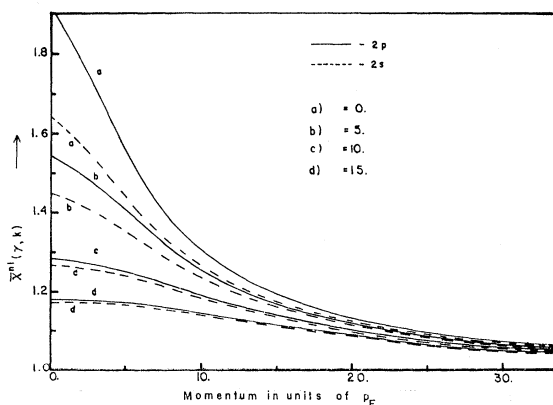


FIG. 1. Solution of the integral equation (5.6) for the amplitude $\bar{X}^{nl}(\gamma, k)$ as a function of momentum k and for a number of γ values. Notice that $\bar{X}^{nl}(\gamma, k)$ is defined only for $k > 1$, i.e., above the Fermi surface.

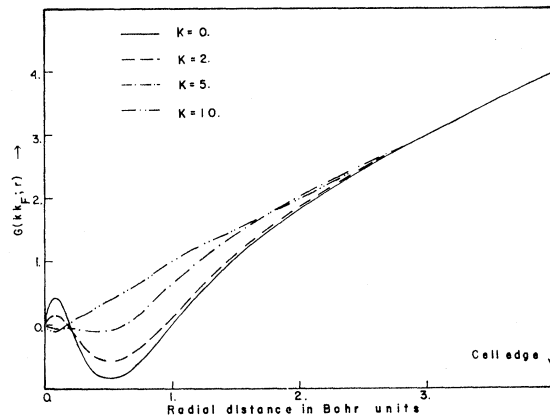


FIG. 2. The k dependence of the quantity $G(k_F k, r)$ entering Eq. (5.4). The complex structure from the orthogonalization parts smooths out for sufficient large k .

represents a less serious perturbation in this case. Smaller enhancement factors should result. They are nevertheless significant.

The starting point of this paper will be the formula for core annihilation obtained in Ref. 1 within the ladder scheme. As derived, this formula is valid only for simple metals so that we will limit the discussion to sodium and aluminum. In these metals the core functions do not overlap appreciably and a single orthogonalized plane wave (OPW) gives a reasonable description of the conduction band. In Sec. II, the basic expression for core annihilation is first described in some detail and then simply written down. Contact with the conventional I.P.M. of Berko and Plaskett is made. Section II is concerned mainly with the necessary preliminaries to the evaluation of the correlation correction to the I.P.M. In particular, the OPW's for the conduction band are introduced. The expression for core annihilation is reduced to a form appropriate for numerical work in Sec. IV. A number of approximations are necessary to make the work tractable but we believe these not to be critical. The numerical work is described in Sec. V where some of the intermediate results are also presented. The enhancement factors obtained are given in Sec. VI where we draw conclusions and compare theory with experiment.

II. FORMULA FOR THE PARTIAL RATE $R[\mathbf{p}]$

The prescription for the partial rate $R[\mathbf{p}]$ (i.e., annihilation with emission of a γ -ray pair of total momentum \mathbf{p}), derived in Ref. 1 for core electrons, can be described as follows. It is proportional to the absolute square of the sum of two terms; the first gives the I.P.M. result and is the p th Fourier component of the core electron and positron single-particle wave-function overlap. The second term is a correction which describes at least approximately, the correlation in the relative motion of the annihilating pair. Although the structure

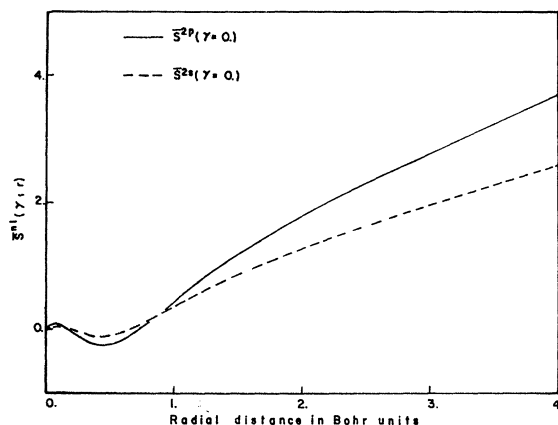


FIG. 3. The function $S^{nl}(\gamma; r)$ for the $2p$ and $2s$ shell.

of this contribution is fairly complicated, it can still be understood in a qualitative way.

First, it is proportional to a matrix element between a single-particle core state and an unoccupied conduction state. This matrix element arises because of the possible virtual excitation of the core electron to the available states above the Fermi surface induced by the positron force. The positron must of course "follow along" and hence there should also appear in the expression for $R[\mathbf{p}]$ a positron-positron matrix element describing a transition from the lowest-energy Bloch state to an excited state. This matrix element, however, can be evaluated with little error using plane waves and hence does not appear explicitly in $R[\mathbf{p}]$. Alternatively, one can think of it as having been absorbed in the enhancement factor which multiplies the basic conduction-core matrix element. This enhancement factor further contains the screened electron-positron potential causing the various transitions and appropriate energy denominators.

If one were content to treat the electron-positron attraction in Born approximation, it would not be necessary to solve an integral equation for the enhancement factor. Unfortunately, this is not justified.¹ The necessary integral equation is, however, relatively simple because it refers only to further repeated scatterings of the annihilating pair once the electron has made a transition to the unoccupied part of the conduction band as a result of a first interaction. Only conduction-conduction matrix elements enter in the description of such further scatterings. These can again be evaluated with only minor errors using plane waves at least for simple metals.

The work of Ref. 1 will not be discussed further here. It is hoped that the above brief description of the basic expression for core annihilation is sufficient to convince the reader of the reasonableness of the starting formula which we now specify in detail. The contribution to the partial annihilation rate $R[\mathbf{p}]$ from a core electron in the state $[nlm; \mathbf{s}]$ (where the nl index refers to the

band, m is the magnetic quantum number, and \mathbf{s} is the crystal momentum restricted to the first Brillouin zone) is given by

$$R^{[nlm; \mathbf{s}]}[\mathbf{p}] = (\lambda/V) | I_{[nlm; \mathbf{s}]}(\mathbf{p}) + V^{-1} \sum_{\mathbf{k}} \epsilon_p^{nl}(\mathbf{k}) [\mathbf{k} | \mathbf{p} - \mathbf{k} | nlm; \mathbf{s}]^e |^2, \quad (2.1)$$

where

$$I_{[nlm; \mathbf{s}]}(\mathbf{p}) = \int \Psi_{[nlm; \mathbf{s}]}(\mathbf{x}) [\exp(-i\mathbf{p} \cdot \mathbf{x})] \Phi_0(\mathbf{x}) d^3x \quad (2.2)$$

and

$$[\mathbf{k} | \mathbf{p} - \mathbf{k} | nlm; \mathbf{s}]^e = \int \Psi_{[\mathbf{k}]}^*(\mathbf{x}) [\exp(-i(\mathbf{p} - \mathbf{k}) \cdot \mathbf{x})] \Psi_{[nlm; \mathbf{s}]}(\mathbf{x}) d^3x. \quad (2.3)$$

In Eq. (2.1) V is the volume of the crystal and λ is a proportionality constant defined in Ref. 1. The enhancement factor $\epsilon_p^{nl}(\mathbf{k})$ will be specified later. In the electron-positron overlap integral (2.2) $\Psi_{[nlm; \mathbf{s}]}(\mathbf{x})$ is the single-particle Bloch state for the core electron $[nlm; \mathbf{s}]$, and the wave function $\Phi_0(\mathbf{x})$ is the lowest-energy positron Bloch state. In determining $\Phi_0(\mathbf{x})$ the potential seen by the positron in any given Wigner-Seitz cell is taken to be the sum of the Hartree field of the ion core in that cell, of net charge Z , plus the potential coming from Z conduction electrons uniformly smeared throughout the cell, so as to neutralize it. Treating only this first term in (2.1) leads to the Berko-Plaskett theory of core annihilation.

In the electron-electron matrix element (2.3), $\Psi_{[\mathbf{k}]}(\mathbf{x})$ stands for an unoccupied state in the conduction band which we will describe by a single orthogonalized plane wave (OPW). The sum over the momentum label \mathbf{k} in (2.1) extends over all possible such unoccupied states, i.e., over all OPW's $|\mathbf{k}\rangle$ with $|\mathbf{k}|$ greater than the

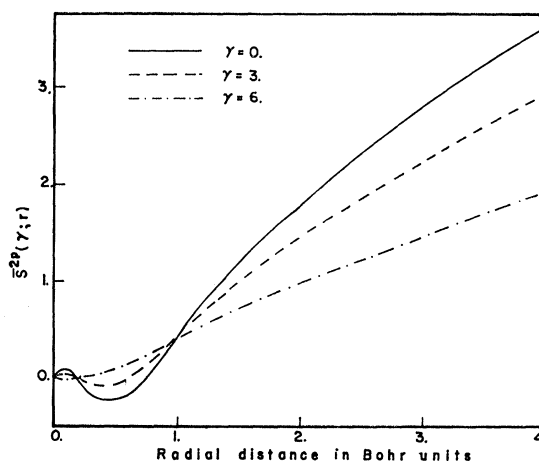


FIG. 4. The γ dependence of the function $S^{nl}(\gamma; r)$ for the $2p$ shell. The lack of oscillations implies that the correlation corrections have much the same variation with r as the I.P.M. term.

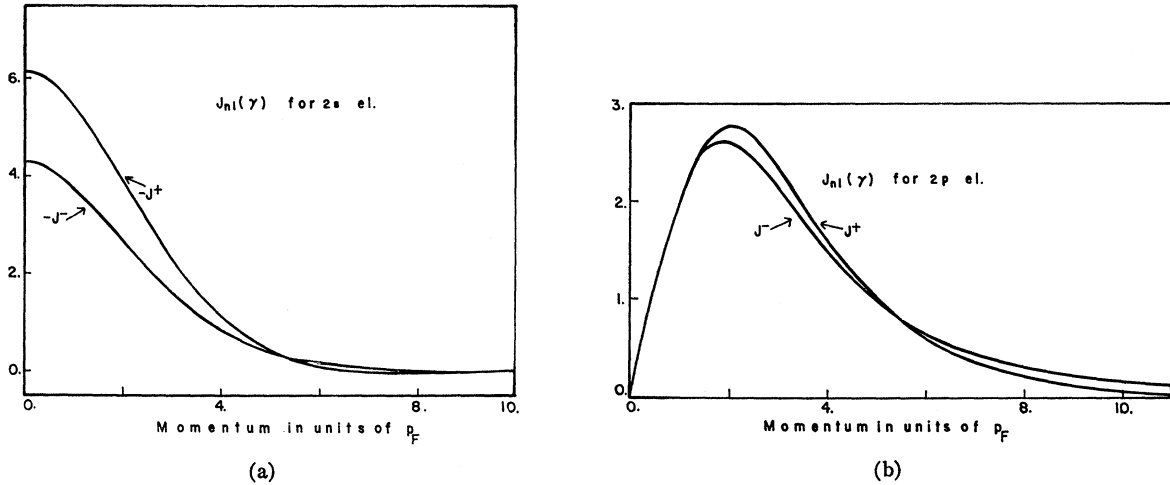


FIG. 5. The overlap integrals $J_{nl}^{\pm}(\gamma)$ for the 2s (a) and 2p (b) electronic shells showing the similarity of the J^- to the J^+ term.

Fermi momentum k_F . The enhancement factor $\epsilon_p^{nl}(\mathbf{k})$ multiplying the matrix element (2.3) in Eq. (2.1) can be written in the form

$$\epsilon_p^{nl}(\mathbf{k}) = X_p^{nl}(\mathbf{k}) \frac{\theta(k - k_F)}{k^2 + (\mathbf{p} - \mathbf{k})^2 + \Delta_{nl}} u_s(\mathbf{p} - \mathbf{k}), \quad (2.4)$$

where the amplitude $X_p^{nl}(\mathbf{k})$ in general, satisfies an integral equation. Treating the electron-positron scattering process in Born approximation, however, corresponds to taking $X_p^{nl}(\mathbf{k}) = 1$. In Eq. (2.4), we are using units such that $\hbar = 2m = 1$. Also, we have made a quadratic approximation for the single-particle energy associated with the OPW $|\mathbf{k}\rangle$. A similar approximation was used to describe the positron energy at the bottom of the 1s band. The parameter Δ_{nl} , appearing in the energy denominator of (2.4), is just the energy gap between the nl core level and the bottom of the 3s conduction band. The theta function $\theta(k - k_F)$ is a step function of value 1 for $k > k_F$ and 0 otherwise. This ensures that the only allowed electronic transitions are to OPW's above the Fermi surface. Finally, the potential function $u_s(\mathbf{q})$ appearing in (2.4) is the zero-frequency component of the space-time Fourier transform of the effective electron-positron force in the random-phase approximation.

The prescription for core annihilation derived in Ref. 1, which is the basis of this paper, is now completely specified provided the amplitude $X_p^{nl}(\mathbf{k})$ is known. It satisfies the integral equation

$$X_p^{nl}(\mathbf{k}) = 1 + \frac{1}{V} \sum_{\mathbf{k}'} X_p^{nl}(\mathbf{k}') \frac{\theta(k' - p_F)}{k'^2 + (\mathbf{p} - \mathbf{k}')^2 + \Delta_{nl}} \times u_s(\mathbf{k} - \mathbf{k}'). \quad (2.5)$$

The task now is to evaluate (2.1). The most awkward part is to make a reasonable calculation of the core-conduction matrix element (2.3). This difficulty arises

because core functions are largest where conduction-state wave functions are smallest and vice versa.

For the core function $\Psi_{[nlm;s]}(\mathbf{x})$ we can use a tight-binding sum

$$\Psi_{[nlm;s]}(\mathbf{x}) = N^{-1/2} \sum_{\mathbf{R}_\nu} \exp(i\mathbf{s} \cdot \mathbf{R}_\nu) U_{nlm}(\mathbf{x} - \mathbf{R}_\nu), \quad (2.6)$$

where N is the number of primitive cells in the crystal while the \mathbf{R}_ν vectors specify their positions in space. The atomiclike wave function $U_{nlm}(\mathbf{x})$ centered about $\mathbf{x} = 0$ can be written as

$$U_{nlm}(\mathbf{x}) = [P_{nl}(r)/r] Y_{lm}(\hat{x}),$$

where $Y_{lm}(\hat{x})$ is the (lm) th spherical harmonic referred, for the moment, to some general coordinate system, and $P_{nl}(r)/r$ is the radial part of the core wave function. The $P_{nl}(r)$ were taken from the Hartree-Fock-Slater calculation by Taylor.⁹ Introducing the tight-binding sum (2.6) into Eq. (2.1) yields

$$R^{[nlm;s]}[\mathbf{p}] = \frac{\lambda}{V} \left| \left(\frac{N}{V} \right)^{1/2} \delta_{\mathbf{s}-\mathbf{p},\kappa} \int d^3x U_{nlm}(\mathbf{x}) \exp(-i\mathbf{p} \cdot \mathbf{x}) \times [v_0(\mathbf{x}) + V^{-1} \sum_{\mathbf{k}} \epsilon_p^{nl}(\mathbf{k}) u_{\mathbf{k}}^*(\mathbf{x})] \right|^2, \quad (2.7)$$

where κ is a reciprocal lattice vector and the functions $v_0(\mathbf{x})$ and $u_{\mathbf{k}}(\mathbf{x})$ have their usual meaning, namely

$$\Phi_0(\mathbf{x}) = (1/V^{1/2}) v_0(\mathbf{x})$$

and

$$\Psi_{[\mathbf{k}]}(\mathbf{x}) = (1/V^{1/2}) \exp(i\mathbf{k} \cdot \mathbf{x}) u_{\mathbf{k}}(\mathbf{x}).$$

Denoting by $R^{nl}[\mathbf{p}]$ the contribution to the partial annihilation rate coming from the sum of all the core

⁹ Roger Taylor (private communication).

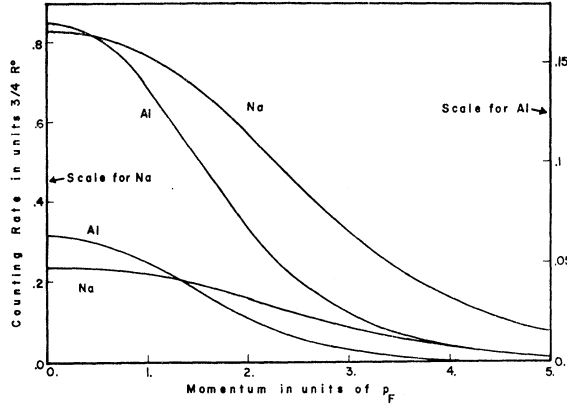


FIG. 6. The contribution of the core electrons to the two-photon counting rate for both Na and Al. The enhanced curves are nearly simple multiples of the I.P.M. curves.

electrons in the nl band we get from (2.7)

$$R^{nl}[\mathbf{p}] = \sum_{m=-l}^l R^{[nlm;sl]}[\mathbf{p}]$$

$$= \frac{\lambda}{V} \frac{1}{\Omega^0} \sum_{m=-l}^l \left| \int d^3x U_{nlm}(\mathbf{x}) \exp(-i\mathbf{p}\cdot\mathbf{x}) \right.$$

$$\left. [v_0(\mathbf{x}) + V^{-1} \sum_{\mathbf{k}} \epsilon_p^{nl}(\mathbf{k}) u_{\mathbf{k}}^*(\mathbf{x})] \right|^2, \quad (2.8)$$

where Ω^0 is the volume of a primitive lattice cell and Ω^0/Z is the volume per conduction electron.

III. $R[\mathbf{p}]$ ON A ONE OPW MODEL

The second term appearing in formula (2.8) represents a correction to the Berko-Plaskett theory due to correlations between the annihilating pair. To evaluate it one needs to know the single-particle states for the conduction as well as higher bands. For metals like sodium and aluminum, it is generally accepted that a single OPW gives a reasonable description of these states. Such wave functions are plane waves to which one adds a core admixture so as to make them orthogonal to all core functions. We can write

$$|\text{OPW}:\mathbf{k}\rangle = N_k^{-1} [V^{-1/2} \exp(i\mathbf{k}\cdot\mathbf{x}) - \sum_{n'l'm'} B_{n'l'm';\mathbf{k}} \Psi_{[n'l'm';\mathbf{k}]}(\mathbf{x})], \quad (3.1)$$

where N_k is a normalization factor determined by insisting that

$$\langle \mathbf{k}:\text{OPW} | \text{OPW}:\mathbf{k} \rangle = 1. \quad (3.2)$$

In Eq. (3.1) the $B_{n'l'm';\mathbf{k}}$'s are called the orthogonalization coefficients and the $\Psi_{[n'l'm';\mathbf{k}]}(\mathbf{x})$'s are the tight-binding sums for the core electrons as previously defined except that it is now convenient to use an *extended* rather than a *reduced* zone scheme on the momentum index \mathbf{k} which is now unrestricted. Orthogonaliza-

tion of the OPW to the core states is achieved by requiring that

$$\langle \Psi_{[nlm;\mathbf{k}]} | \text{OPW}:\mathbf{k}' \rangle = 0. \quad (3.3)$$

For $\mathbf{k}' \neq \mathbf{k} \pm \boldsymbol{\kappa}$, where $\boldsymbol{\kappa}$ is any inverse lattice vector, condition (3.3) is automatically satisfied because of momentum conservation. Since from (2.6) it is clear that $\Psi_{[nlm;\mathbf{k} \pm \boldsymbol{\kappa}]} \equiv \Psi_{[nlm;\mathbf{k}]}$, we need only consider the case $\mathbf{k}' = \mathbf{k}$. For a metal in which cores do not overlap significantly, condition (3.3) then reduces to

$$B_{n'l'm';\mathbf{k}} = \frac{1}{\Omega_0^{1/2}} \int d^3y U_{n'l'm'}^*(\mathbf{y}) \exp(i\mathbf{k}\cdot\mathbf{y}). \quad (3.4)$$

To evaluate this integral, it is convenient to make a spherical harmonic expansion of the exponential

$$\exp(i\mathbf{k}\cdot\mathbf{x}) = \sum_{l'm'} 4\pi (i)^{l'} Y_{l'm'}(\hat{\mathbf{k}}) j_{l'}(kr) Y_{l'm'}^*(\hat{\mathbf{x}}), \quad (3.5)$$

where the spherical harmonics $Y_{l'm'}$ are to be referred to the same general coordinate system as that used to write down the core functions $U_{nlm}(\mathbf{x})$ in the previous section. In (3.5) the j_l 's are the spherical Bessel functions of order l . Substituting expression (3.5) into (3.4) gives

$$B_{n'l'm';\mathbf{k}} = 4\pi (i)^{l'} Y_{l'm'}^*(\hat{\mathbf{k}}) A_{n'l'}(k) \quad (3.6)$$

with

$$A_{n'l'}(k) = \frac{1}{\Omega_0^{1/2}} \int_0^\infty r dr j_{l'}(kr) P_{n'l'}(r), \quad (3.7)$$

which defines the orthogonalization coefficients as integrals over the core Hartree-Fock-Slater functions.

The normalization condition (3.2) can easily be expressed in terms of the coefficients $A_{n'l'}(k)$. After some simple algebra involving the completeness sum for spherical harmonics

$$\frac{2l'+1}{4\pi} = \sum_{m'=-l'}^{l'} Y_{l'm'}(\hat{\mathbf{x}}) Y_{l'm'}^*(\hat{\mathbf{x}}), \quad (3.8)$$

we find

$$|N_k|^2 = 1 - \sum_{n'l'} 4\pi (2l'+1) |A_{n'l'}(k)|^2. \quad (3.9)$$

The OPW (3.1) is now completely defined and the corresponding reduced wave function $u_{\mathbf{k}}(\mathbf{x})$ can be expanded to read

$$u_{\mathbf{k}}(\mathbf{x}) = \frac{1}{N_k} [1 - 4\pi \Omega_0^{1/2} \sum_{\mathbf{R}_\nu} \sum_{n'l'm'} (i)^{l'} \times \exp[-i\mathbf{k}\cdot(\mathbf{x}-\mathbf{R}_\nu)] Y_{l'm'}^*(\hat{\mathbf{k}}) A_{n'l'}(k) U_{n'l'm'}(\mathbf{x}-\mathbf{R}_\nu)], \quad (3.10)$$

where use was made of Eqs. (2.6) and (3.6).

Note that the atomiclike function $U_{nlm}(\mathbf{x})$ enters as a multiplicative factor. Since we have assumed this function to be well localized inside the Wigner-Seitz cell, we will need $u_{\mathbf{k}}(\mathbf{x})$ only about $x=0$, i.e., only in the primitive lattice cell defined by $\mathbf{R}_\nu=0$. Thus, we need retain only the first term in the lattice sum ($\sum \mathbf{R}_\nu$) appearing in Eq. (3.10); for \mathbf{x} about the origin then

$$u_{\mathbf{k}}(\mathbf{x}) = \frac{1}{N_k} [1 - 4\pi\Omega_0^{1/2} \exp(-i\mathbf{k}\cdot\mathbf{x}) \sum_{n'l'm'} (i)^l Y_{l'm'}^*(\hat{k}) \times A_{n'l'}(k) U_{n'l'm'}(\mathbf{x})]. \quad (3.11)$$

Substituting this last expression into the second term of (2.8) yields

$$V^{-1} \sum_{\mathbf{k}} \epsilon_p^{nl}(\mathbf{k}) u_{\mathbf{k}}^*(\mathbf{x}) = V^{-1} \sum_{\mathbf{k}} \epsilon_p^{nl}(\mathbf{k}) \frac{1}{N_k} [1 - 4\pi\Omega_0^{1/2} \times \exp(i\mathbf{k}\cdot\mathbf{x}) \sum_{n'l'm'} (-i)^l Y_{l'm'}^*(\hat{k}) A_{n'l'}^*(k) U_{n'l'm'}^*(\mathbf{x})]. \quad (3.12)$$

A great simplification would occur in this last equation if we replaced the enhancement factor $\epsilon_p^{nl}(\mathbf{k})$ by its spherical average over the angles of \mathbf{k} since it would then be possible to use the angular integration $d\Omega_{\mathbf{k}}$ to simplify the second term in (3.12). This approximation seems intuitively reasonable since one does not expect the enhancement factor $\epsilon_p^{nl}(\mathbf{k})$ to have a strong directional dependence on the vector \mathbf{k} . In any case, retaining this directional dependence would make the final numerical work painfully complex. For the moment, we propose to simply make the necessary spherical average. Its effect on the calculation will become clear later. It is worth pointing out in passing however, that the procedure is exact for the first term in the square bracket of (3.12) so that we are treating, in this approximate way, only the orthogonalization corrections. Incorporating this idea into Eq. (3.12) yields

$$V^{-1} \sum_{\mathbf{k}} \epsilon_p^{nl}(\mathbf{k}) u_{\mathbf{k}}^*(\mathbf{x}) = V^{-1} \sum_{\mathbf{k}} \epsilon_p^{nl}(\mathbf{k}) N_k^{-1} [1 - \Omega_0^{1/2} \times \sum_{n'l'm'} (-i)^l \left\langle \int d\Omega_{\mathbf{k}} \exp(i\mathbf{k}\cdot\mathbf{x}) Y_{l'm'}(\hat{k}) \right\rangle \times A_{n'l'}^*(k) U_{n'l'm'}^*(\mathbf{x})], \quad (3.13)$$

where it was not necessary to introduce explicitly the spherical average of the enhancement factor. Expanding the plane wave $\exp(i\mathbf{k}\cdot\mathbf{x})$ that remains in (3.13) according to Eq. (3.5), one obtains for the right-hand side

$$V^{-1} \sum_{\mathbf{k}} \epsilon_p^{nl}(\mathbf{k}) [1 - \Omega_0^{1/2} \times \sum_{n'l'm'} 4\pi Y_{l'm'}(\hat{x}) j_l(kr) A_{n'l'}^*(k) U_{n'l'm'}^*(\mathbf{x})] N_k^{-1}. \quad (3.14)$$

Finally writing out more explicitly the core function $U_{n'l'm'}(\mathbf{x})$ in (3.14), and making use of the complete-

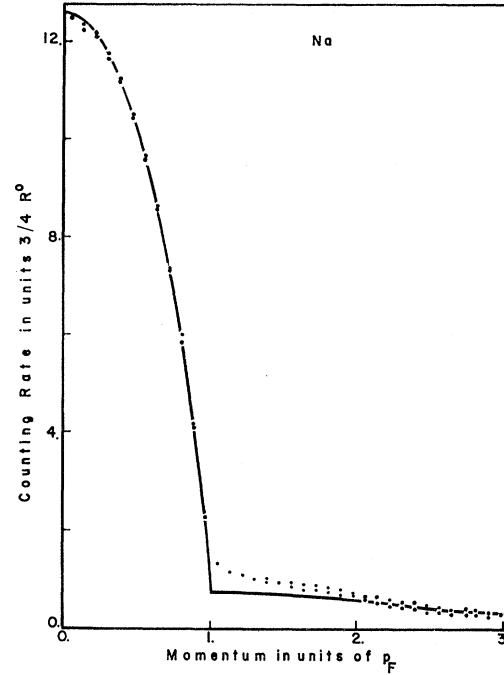


FIG. 7. The two-photon counting rate for Na. The experimental data have not been corrected for background effects.

ness sum (3.8) we get

$$V^{-1} \sum_{\mathbf{k}} \epsilon_p^{nl}(\mathbf{k}) N_k^{-1} [1 - (\Omega^0)^{1/2} \times \sum_{n'l'} (2l'+1) j_{l'}(kr) A_{n'l'}^*(k) (P_{n'l'}(r)/r)]. \quad (3.15)$$

It is convenient in what follows to write (3.15) in a more compact form by introducing the quantity

$$G(k; r) = r - (\Omega^0)^{1/2} \sum_{n'l'} (2l'+1) j_{l'}(kr) A_{n'l'}^*(k) P_{n'l'}(r). \quad (3.16)$$

This gives

$$V^{-1} \sum_{\mathbf{k}} \epsilon_p^{nl}(\mathbf{k}) u_{\mathbf{k}}^*(\mathbf{x}) = V^{-1} \sum_{\mathbf{k}} \epsilon_p^{nl}(\mathbf{k}) N_k^{-1} [G(k; r)/r]. \quad (3.17)$$

IV. ALGEBRAIC REDUCTION

Substitution of the result (3.17) into the expression (2.8) for the partial rate $R^{nl}[\mathbf{p}]$ resulting from annihilation with electrons in the nl core band gives

$$R^{nl}[\mathbf{p}] = (\lambda/V) \Omega_0^{-1} \sum_{m=-l}^l \left| \int d^3x [P_{nl}(r)/r] Y_{lm}(\hat{x}) \times \exp(-i\mathbf{p}\cdot\mathbf{x}) [v_0(\mathbf{x}) + V^{-1} \times \sum_{\mathbf{k}} \epsilon_p^{nl}(\mathbf{k}) N_k^{-1} G(k; r)/r] \right|^2. \quad (4.1)$$

The function $v_0(\mathbf{x})$ is the positron Bloch state at the

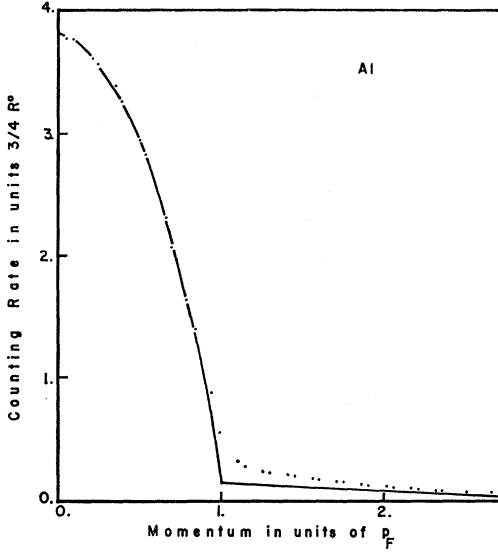


FIG. 8. The two-photon counting rate for Al.

bottom of the 1s band and is needed only in the Wigner-Seitz sphere about $\mathbf{R}_v=0$. Thus we can take it to be spherically symmetric and write it in the form $R^+(r)/r$. Noting that the entire expression in the small square brackets of (4.1) depends only on the $|\mathbf{x}|=r$, the angular integration can be performed. The result is

$$R^{nl}[\mathbf{p}] = (\lambda/V)\Omega_0^{-1} \sum_{m=-l}^l 4\pi (-i)^l Y_{lm}(\hat{p}) \times \int_0^\infty dr j_l(pr) P_{nl}(r) \times [R_0^+(r) + V^{-1} \sum_{\mathbf{k}} \epsilon_p^{nl}(\mathbf{k}) N_{\mathbf{k}}^{-1} G(k; r)]^2. \quad (4.2)$$

By squaring out (4.2) explicitly and summing over the magnetic quantum number m , one obtains with reference to the sum rule (3.8)

$$R^{nl}[\mathbf{p}] = (\lambda/V)\Omega_0^{-1} 2(2l+1) 4\pi \left| \int_0^\infty dr j_l(pr) P_{nl}(r) \times [R_0^+(r) + V^{-1} \sum_{\mathbf{k}} \epsilon_p^{nl}(\mathbf{k}) N_{\mathbf{k}}^{-1} G(k; r)] \right|^2, \quad (4.3)$$

where the extra factor of 2 accounts for spin degeneracy among the core levels.

At this point, it is convenient to examine more critically, the angular average of $\epsilon_p^{nl}(\mathbf{k})$ performed in the previous section. It is clear from the integral equation (2.5) for the amplitude $X_p^{nl}(\mathbf{k})$, that while in general it depends on both the vector \mathbf{p} and the vector \mathbf{k} , its most important part goes like 1, which corresponds to Born approximation. In this case (2.4) reduces to

$$\epsilon_p^{nl}(\mathbf{k}) = \frac{\theta(k-k_F)}{k^2 + (\mathbf{p}-\mathbf{k})^2 + \Delta_{nl}} u_s(\mathbf{p}-\mathbf{k}). \quad (4.4)$$

We first note that for $\mathbf{p}=0$, the enhancement factor (4.4) depends only on the magnitude of the vector \mathbf{k} . Further, in the large- \mathbf{p} limit, specifically for $|\mathbf{p}|$ much greater than the absolute value of any vector \mathbf{k} of interest, the angular average over \mathbf{k} of the previous section is again nearly exact. In the intermediate region, the procedure deteriorates and it is difficult to make a quantitative estimate of the error introduced. From the preceding discussion, it may be expected not to be too serious. In any case, it would be very difficult to do better at present.

To average (4.4) over the angles of \mathbf{k} , we take the polar axis along the direction of \mathbf{p} . This gives

$$\int d\Omega_{\mathbf{k}} \epsilon_p^{nl}(\mathbf{k}) = 2\pi\theta(k-k_F) \int_{|p-k|}^{p+k} \frac{z dz}{k^2+z^2+\Delta_{nl}} \frac{u_s(z)}{pk}. \quad (4.5)$$

In practice we really need to solve the integral equation (2.5) for the amplitude $X_p^{nl}(\mathbf{k})$ rather than assume it to be 1 as we have done in (4.4). It should be clear, however, that it would not be consistent to consider any further angular dependence that might be picked up in this way since these are higher-order corrections in the perturbation expansion. As will be seen explicitly in the next section, these higher terms have the effect of changing the number 1 to a number between 2 and 1 but for the most part considerably less than 2. To solve (2.5) we will then simply assume $X_p^{nl}(\mathbf{k})$ to depend only on the $|\mathbf{p}|$ and $|\mathbf{k}|$.

We now put together the results obtained so far. From the definition of the enhancement factor (2.4), and the idea that the amplitude $X_p^{nl}(\mathbf{k})$ can depend in an important way only on $|\mathbf{p}|$ and $|\mathbf{k}|$, Eq. (4.3) can be rewritten in the form

$$R^{nl}[\mathbf{p}] = (\lambda/V)\Omega_0^{-1} 2(2l+1) 4\pi \left| \int_0^\infty dr j_l(pr) P_{nl}(r) \times \left[R_0^+(r) + \int \frac{k^2 dk}{(2\pi)^3} \theta(k-k_F) \chi^{nl}(p, k) N_{\mathbf{k}}^{-1} G(k; r) \times \int_{|p-k|}^{p+k} \frac{2\pi z dz}{k^2+z^2+\Delta_{nl}} \frac{u_s(z)}{pk} \right] \right|^2, \quad (4.6)$$

where use was made of Eq. (4.5). Also, for convenience, we have taken the limit of infinite volume. The quantity $\chi^{nl}(p, k)$ stands for the solution of the integral equation

$$\chi^{nl}(p, k) = 1 + \int \frac{d^3 k'}{(2\pi)^3} \theta(k'-k_F) \chi^{nl}(p, k') \times \frac{u_s(\mathbf{k}-\mathbf{k}')}{k'^2 + (\mathbf{p}-\mathbf{k}')^2 + \Delta_{nl}}, \quad (4.7)$$

which was obtained from (2.5) by "blindly" imposing the requirement that the amplitude $X_p^{nl}(\mathbf{k})$ depend only on the absolute value of the two vectors \mathbf{p} and \mathbf{k} . As

written, (4.7) is not consistent. This can be seen trivially by taking the first iterate of (4.7), a quantity that clearly has an angular dependence. This defect can be corrected by either averaging the integrand over the angles of \mathbf{p} or alternatively over the angles of \mathbf{k} . It is comforting that both procedures lead to the same integral equation namely,

$$\chi^{nl}(p, k) = 1 + (2pk)^{-1} \int_{k_F}^{\infty} dk' K_p^{nl}(k, k') \chi^{nl}(p, k') \quad (4.8)$$

with the kernel $K_p^{nl}(k, k')$ given by

$$K_p^{nl}(k, k') = \frac{1}{(2\pi)^2} \int_{|k-k'|}^{k+k'} zdz \frac{1}{2} u_s(z) \times \ln \left[\frac{k'^2 + (p+k')^2 + \Delta_{nl}}{k'^2 + (p-k')^2 + \Delta_{nl}} \right]. \quad (4.9)$$

We are now in a position to discuss the numerical evaluation of $R^{nl}[\mathbf{p}]$ as given by Eq. (4.6). This is the subject of the next section.

V. NUMERICAL EVALUATION

It is convenient to denote the second term in (4.6) by $S^{nl}(p; r)$,

$$R^{nl}[\mathbf{p}] = 2(2l+1) \frac{4\pi}{V} (R^0/Z) \left| \int_0^{\infty} dr j_l(pr) P_{nl}(r) \times [R_0^+(r) + S^{nl}(p; r)] \right|^2, \quad (5.1)$$

where $R^0 \equiv \lambda Z / \Omega_0$ is the Sommerfeld annihilation rate. In (5.1) $S^{nl}(p, r)$ stands for

$$S^{nl}(p; r) = \int_{k_F}^{\infty} \frac{k^2 dk}{(2\pi)^3} \chi^{nl}(p, k) N_{k_F}^{-1} G(k; r) \times \int_{|p-k|}^{p+k} \frac{2\pi z dz}{k^2 + z^2 + \Delta_{nl}} \frac{u_s(z)}{pk}. \quad (5.2)$$

We now measure all momenta in units of the Fermi momentum p_F . In particular we write $\mathbf{p} = \gamma p_F$. We get

$$R^{nl}[\gamma p_F] = 2(2l+1) \frac{4\pi}{V} (R^0/Z) \left| \int_0^{\infty} dr j_l(\gamma p_F r) P_{nl}(r) \times [R_0^+(r) + \bar{S}^{nl}(\gamma; r)] \right|^2, \quad (5.3)$$

with

$$\bar{S}^{nl}(\gamma; r) = \int_1^{\infty} \frac{k dk}{\gamma} \bar{\chi}^{nl}(\gamma, k) N_{k p_F}^{-1} \langle G(k p_F; r) \rangle \times \int_{|k-\gamma|}^{k+\gamma} \frac{2\pi z dz \alpha U(z)}{k^2 + z^2 + \phi^{nl}}, \quad (5.4)$$

where $\phi^{nl} \equiv \Delta^{nl} / p_F^2$, $\alpha = r_s / (1.919\pi^2)$ with r_s the usual electron-gas density parameter and the potential function $U(q)$ is

$$U(q) = 1 / \left[q^2 + 2\pi\alpha \left\{ 1 - (2q)^{-1} \left(1 - \frac{1}{4}q^2 \right) \ln \left(\frac{q-2}{q+2} \right)^2 \right\} \right]. \quad (5.5)$$

The integral equation satisfied by $\bar{\chi}^{nl}(\gamma, k) \equiv \chi^{nl}(p_F \gamma, p_F k)$ is from (4.8)

$$\bar{\chi}^{nl}(\gamma, k) = 1 + \int_1^{\infty} \frac{dk'}{2\gamma k} \bar{K}_{\gamma}^{nl}(k, k') \bar{\chi}^{nl}(\gamma, k'), \quad (5.6)$$

with the kernel $\bar{K}_{\gamma}^{nl}(k, k')$ given by

$$\bar{K}_{\gamma}^{nl}(k, k') = \int_{|k-k'|}^{k+k'} zdz \alpha U(z) \pi \ln \left[\frac{k'^2 + (\gamma+k')^2 + \phi^{nl}}{k'^2 + (\gamma-k')^2 + \phi^{nl}} \right]. \quad (5.7)$$

In what follows, we shall discuss in some detail only the results for sodium. Aluminum is not very different. The integral equation (5.6) for a fixed γ was solved by changing it to a set of inhomogeneous linear algebraic equations and using a Gauss elimination technique. The solution for four values of γ are shown in Fig. 1. We give curves only for the $2p$ and $2s$ electrons. The $1s$ band contributes negligibly in comparison. Since the band gap for the $2p$ electrons is less than that for the $2s$, $\bar{\chi}^{2p}(\gamma, k)$ (as a function of k) is always above $\bar{\chi}^{2s}(\gamma, k)$. For large k both tend towards the common value of 1. This behavior is expected as seen most easily from the form of Eq. (4.7). Also, as γ increases, the amplitude $\bar{\chi}$ decreases. It is worth noting, in passing, that we have plotted $\bar{\chi}$ for rather large values of k . An important feature of our calculations is that values of momentum k up to approximately $k=50$, enter in a significant way in the integral (5.4) defining the function $\bar{S}^{nl}(\gamma; r)$.

The quantity $G(k p_F; r)$ entering Eq. (5.4) is plotted in Fig. 2 as a function of the radial distance r in the Wigner-Seitz cell, for four different values of momentum k . Although only k 's greater than 1 enter in the calculation of $\bar{S}^{nl}(\gamma; r)$, the case $k=0$ serves as a check on the calculation. It is well known that at the bottom of the $3s$ band the OPW wave function reduces very nearly to the Wigner-Seitz wave function. On comparing with Callaway's¹⁰ result, this was found to indeed be the case. As k increases, the minimum in the wave function around $r=0.5$ a.u. becomes more shallow since the orthogonalization coefficients in (3.16) rapidly become negligible. For sufficiently large k 's the straight-line part (of slope one) of $G(k p_F; r)$ dominates even for relatively small values of r . For r 's around the cell edge, $G(k p_F; r)$ becomes independent of k and behaves like a straight line because the core functions $P_{n'l'}(r)$ in (3.16) become negligibly small. Thus, deviations

¹⁰ J. Callaway, Phys. Rev. **123**, 1255 (1961).

from a straight-line behavior occurs only for small r 's and k 's.

Noting from Fig. 2 that the difference between $G(k_F k; r)$ at $k=0$ and $k=2.5$ is not great, it is easy to see that if the only transitions of importance in (5.4) were those about the Fermi surface, i.e., $k=1$ we would recover the model discussed in Ref. 1. This results because it would then be justified to fix $G(k_F k; r)$ in (5.4) at $G(k_F; r)$ and pull it out of the k integral. But $G(k_F; r)$ is nearly equal to $G(0; r)$ which in turn reduces to the Callaway wave function $R_0(r)$ so that

$$\bar{S}^{nl}(\gamma; r) \cong R_0^-(r) m^{nl}(\gamma), \quad (5.8)$$

with

$$m^{nl}(\gamma) = \int_1^\infty \frac{k dk}{\gamma} \bar{\chi}^{nl}(\gamma, k) \int_{|k-\gamma|}^{k+\gamma} \frac{2\pi z dz \alpha U(z)}{k^2 + z^2 + \phi^{nl}}, \quad (5.9)$$

where $m^{nl}(\gamma)$ is essentially the same quantity as that plotted in Fig. 5 of Ref. 1. This procedure is however, not justified. We have seen that the amplitude $\bar{\chi}^{nl}(\gamma, k)$ does not have a strong k variation. Also, the quantity

$$k \int_{|k-\gamma|}^{k+\gamma} \frac{2\pi z dz \alpha U(z)}{k^2 + z^2 + \phi^{nl}} \equiv A(k) \quad (5.10)$$

is not a rapidly damping function about the Fermi surface. This means that $G(k k_F; r)$'s for many values of k get averaged over in the expression for $\bar{S}^{nl}(\gamma; r)$. Since for large k 's the $G(k k_F; r)$'s are nearly straight lines (as a function of r), the dip at $r \cong 0.5$ a.u. occurring in $G(k k_F; r)$ for k around 1 will clearly be considerably smoothed out in $\bar{S}^{nl}(\gamma; r)$. This can be seen in Fig. 3 where we have plotted $\bar{S}^{nl}(0; r)$ for the $2p$ and $2s$ shell. The little structure that remains for small r is reduced even further as γ increases. This is shown in Fig. 4, where the results for the $2p$ shell are plotted for $\gamma=0, 3$, and 6 . The lack of any pronounced wiggles in all these curves implies, of course, that the correlation correction in (5.3) will have much the same variation with γ as the I.P.M. term.

Our final results can perhaps be presented best by introducing as in Ref. 1, the intermediate quantities

$$J_{ni}^+(\gamma) = \int_0^\infty dr j_l(p_F r) P_{ni}(r) R_0^+(r) \quad (5.11a)$$

and

$$J_{ni}^-(\gamma) = \int_0^\infty dr j_l(p_F r) P_{ni}(r) \bar{S}^{nl}(\gamma, r) \quad (5.11b)$$

in terms of which Eq. (5.3) can be written as

$$\begin{aligned} R^{nl}(\gamma p_F) \\ = 2(2l+1)(4\pi/V)(R^0/Z) |J_{ni}^+(\gamma) + J_{ni}^-(\gamma)|^2. \end{aligned} \quad (5.12)$$

The results obtained for the $J_{ni}^\pm(\gamma)$'s are presented in Fig. 5. We see explicitly now that the $J_{ni}^-(\gamma)$'s have very much the same momentum variation as the $J_{ni}^+(\gamma)$'s. In fact, for sodium, the magnitude of these two quantities are nearly equal so that neglecting either

would lead to an underestimate of $R^{nl}(\gamma p_F)$ by roughly a factor of 4. These results are quite different from those obtained on the crude model of Ref. 1. In that work, $J^-(\gamma)$ had quite a distinct momentum variation from $J^+(\gamma)$ and a considerable amount of destructive interference actually occurred between the two. This feature now appears to be mostly due to a defect of the model used.

To end this section, we would like to point out that the calculations so far, can be put to the following check. We have noted previously that for r around the Wigner-Seitz cell edge, $G(k p_F; r)$ behave very nearly like a straight line of slope 1 for arbitrary k . Hence in this region $\bar{S}^{nl}(\gamma; r)$ should go like a straight line of slope $m^{nl}(\gamma)$ provided one assumes the OPW normalization factor $N_{k p_F}$ to be 1. This indeed checks out, as can be verified from Fig. 4 and the value for $m^{nl}(\gamma)$ given in Ref. 1.

VI. DISCUSSION

In an angular correlation experiment one does not measure $R^{nl}[p_F \gamma]$ directly since the usual apparatus is unable to discriminate against two of the three momentum components of the γ -ray pair. Only an average over two components enters, namely,

$$N^{\text{core}}[\gamma_z] = \sum_{n_i} \int d\gamma_x d\gamma_y R^{nl}[p_F \gamma] p_F,$$

where the z direction is defined by the geometry of the instrument. We have summed over all core electrons and the units are such that the counting rate $N^{\text{core}}[\gamma_z]$ integrated over the dimensionless variable γ_z gives the total rate. The results obtained for $N^{\text{core}}[\gamma_z]$ are presented in Fig. 6 for aluminum as well as for sodium. For comparison the I.P.M. results are also plotted. Although, at first sight, the enhanced curve may appear to be quite different from the Berko-Plaskett result, they are actually, very nearly, simple multiples of one another. For sodium the variance in the multiplicative factor is less than 5% throughout, while in aluminum it is slightly more. Thus, the core enhancement factors are almost momentum-independent although quite large. In sodium, the core electrons contribute an amount $3.5R^0$ to the total rate as compared to $0.97R^0$ from the Berko-Blaskett term. The over-all enhancement factor is hence ~ 3.6 which is much larger than the rough estimate of 2.2 made previously, on the basis of a very crude model. The results in aluminum are similar. The total rate is $1.4R^0$ as opposed to $0.49R^0$ on the I.P.M. The average enhancement factor is 2.8 which is substantially less than the sodium result. This seems intuitively correct since the core functions in aluminum are "stiffer" and the screening of the bare electron-positron force is greater.

Strictly speaking we have demonstrated that ladder corrections to the I.P.M. do not change appreciably the shape of the counting rate only in the very simple

cases of Al and Na. It is of some interest to consider the possibility that this result may, in fact, be more general. If so, it would be possible to interpret experimental results in more complicated cases semiphenomenologically on the I.P.M. supplemented by constant core enhancement factors. These could be chosen empirically to give the best possible fit to the angular correlation data as well as lifetimes. In fact, this has been attempted with some success by Berko and Terrell¹¹ for certain ferromagnetic metals in the transition series although discrepancies arise. In particular, they conclude that such a procedure overestimates the high-momentum tails. The experiments favor momentum-dependent enhancement factors decreasing with increasing angle. Our present calculations show no evidence of such a tendency at least in the region (0 to $3p_F$). It is important to realize, however, that the simple considerations of this paper cannot really be applied directly to materials as complicated as ferromagnetic metals. The basic formula used is, in fact, suspected for such cases. Thus Berko and Terrell's limited success is very encouraging. On the other hand, it is worth mentioning that even in the case of Al and Na, experiments seem to favor a nontrivial momentum dependence of core enhancement factors although the evidence is not unambiguous. This discrepancy could be due to a number of causes. We shall mention only a few here. Certainly, the angular average made in the course of the calculation is less accurate in the intermediate- p region than in the zero or large- p limit. A more careful treatment of this region seems, however, to be prohibitively difficult and probably not worthwhile. Perhaps more important, is our neglect of positron self-energy corrections. The work of Woll and Rose,¹² in solid argon, indicates that these can be significant in certain cases and, more important, that they represent shape-dependent corrections. Their considerations, however, cannot be applied directly to core electrons in metals, where it is likely that other corrections to the simple ladder approximation are equally important. Further progress would probably require a systematic study of all the other terms in the perturbation series. This does not seem to be necessary. As we shall now see, the agreement of the present theory with experiment is really quite reasonable and the core enhancement factors obtained in Na and Al are likely to be adequate, at least at this stage of our understanding of the subject. In fact, indications are that uncertainties in present electron-gas calculations are probably much more serious sources of error than any corresponding limitation on core-annihilation computations.

Since the major contribution to the counting rate arises from the conduction electrons, it is necessary to add these onto the results for core annihilation when

¹¹ S. Berko and J. H. Terrell, in *Optical Properties and Electronic Structure of Metals and Alloys*, edited by F. Abelès (John Wiley & Sons, Inc., New York, 1966), p. 210.

¹² E. J. Woll, Jr. and K. L. Rose, *Phys. Rev.* **145**, 268 (1966).

making a comparison with experiment. For the conduction electrons we will use the latest available estimates based on plane-wave theory. In Fig. 7, we present a least-squares fit¹³ to the experimental data of Kim and Stewart¹⁴ in sodium. Only half the angular correlation curve is shown although the data from both sides of the distribution were used in the comparison. The scatter-out in the tail results in part from our use of the raw data uncorrected for background. Also the experiments were not made specifically with this region in mind. For the present comparison, these data are nevertheless adequate. Generally the agreement is good, although as discussed previously out in the tails, the theoretical curve is above the experimental points suggesting that the present theory perhaps predicts too broad a distribution for core annihilation. In the range p_F to $2p_F$, the remaining discrepancy is tentatively assigned to lattice effects in the conduction-electron gas. That this is reasonable can be seen as follows.

It is not difficult to estimate crystal-field corrections to the Sommerfeld parabola using the I.P.M. The more important question of how to enhance the resulting tails is however, as yet, unresolved and appears not to be straightforward. Lacking a fundamental calculation, it seemed to us reasonable to multiply these tails by a smoothly dropping enhancement factor chosen at p_F to be equal to its average value for the central parabola while around $3p_F$ it was constrained to take on its average value for core electrons. In this way, one can obtain a very good fit to the data which is encouraging although the procedure still remains to be justified. One should not exclude the possibility, however, that a detailed calculation of the necessary enhancement factors may well yield a function which drops less rapidly with momentum than present experiments indicate. It seems to us, therefore, that this important question must be settled before one can assess precisely the relative success and limitations of our results. Finally, it is important to compare total rates. Theory gives a total rate of $3.0 \times 10^9 \text{ sec}^{-1}$ while the experimental value of Berko and Weisberg¹⁵ is $\sim 2.94 \times 10^9 \text{ sec}^{-1}$. The agreement is excellent.

Our results in Al are similar and are compared to the data of Kusmiss and Stewart¹⁶ in Fig. 8. On the average, the agreement appears to be somewhat better than in sodium. In particular, far out in the tails the data remains above the computed curve. Again, the remain-

¹³ Only the central parabola was used in the least-square fit. This was thought to be the most reasonable procedure since lattice effects in the conduction-electron gas not included in the theoretical curves must certainly make an additive contribution in the tails. The comparison is therefore not unambiguous and the agreement can be changed somewhat by using a different criterion for the least-squares fit.

¹⁴ S. M. Kim and A. T. Stewart (private communication).

¹⁵ These results are presented in Fig. 4 of an article by J. H. Terrell, H. L. Weisberg, and S. Berko, in *Proceedings of the Positron Annihilation Conference* (Academic Press Inc., New York, 1967).

¹⁶ J. H. Kusmiss and A. T. Stewart (private communication).

ing discrepancy is probably due to orthogonalization parts in the conduction band which we have neglected in our comparison. Thus, the angular correlation data can readily be understood at least qualitatively. The area under the calculated curve is, however, about 25% *too great* to agree with lifetime measurements. It would seem that we have overestimated correlation effects in this case. The difficulty can be traced mainly to electron-gas theory which is used to deal with the conduction electrons. In fact, the best available estimate⁵ gives a total rate, from annihilation with the conduction electrons alone, as large as the observed rate. This is clearly an overestimate by at least 15 to 20%. It should be pointed out, however, that in the region of $r_s \sim 2$ the electron-gas curve obtained for the total rate as a function of the density parameter r_s is a rapidly decreasing function so that much of the discrepancy could be removed by using a slightly larger value of r_s than that employed in this work. It is more likely though, that the calculation scheme of Ref. 5 is not as good in the high-density limit (say $r_s \sim 2$) as for $r_s \sim 5$. The ladder approximation appears to be best at low density where it predicts results which go asymptotically toward singlet positronium. This idea is given further support by the fact that the major difference between the simple ladder approximation of Kahana and the more consistent modified ladder scheme of Bergersen and of Ref. 5 is in the case of Al. For Na the difference found between the two schemes is, relatively, much smaller. Further work on electron-gas theory would clearly be desirable. Also more lifetime measurements in the region of $r_s \sim 2$ would be very helpful.

A few concluding remarks mainly on electron-gas theory may not be inappropriate. The recent beautiful experiments of Stewart's group^{17,18} on positron motion in metals indicate that positrons have an effective mass of about twice the bare mass, with some variation with electron-gas density. As yet it has not been possible to calculate the positron effective mass so as to agree with experiment, although several attempts have been made.^{19,20} It is likely that much of the observed re-

normalization of the bare mass is due to correlations between the positron and the conduction-electron gas. A better understanding of this problem should lead to further development in lifetime calculations. The effect of positron self-energy corrections on the annihilation rate (in an electron gas) have been discussed in the past² although only in a linearized approximation. The same approximation employed by Hamann fails to give the observed positron effective mass.

Further, we should mention here the work of Crowell, Anderson, and Ritchie.²¹ These authors were the first to go beyond the random-phase approximation in treating polarization parts. By applying Hubbard corrections they obtained rates from the simple ladder graphs somewhat smaller than those of Kahana. Such corrections, however, are expected physically to be most important at low densities where present theory is best. Nevertheless with the better understanding of the Hubbard parameter ζ achieved recently, particularly through the work of Geldart and Vosko,²² it would seem reasonable to include such corrections in any further calculation.

Finally, we can state that using the ladder approximation to the electron-positron Green's functions, we have had an encouraging amount of success in interpreting the angular correlation data as well as lifetime in sodium and aluminum. Certainly the approximation yields reasonable enhancement factors for core electrons as well as for conduction electrons. In fact, it is likely that when lattice corrections in the conduction band are applied, a detailed quantitative theory will result in sodium, at least in the region 0 to $2p_F$. This is probably the only region of interest since it would show clearly how the main parabolic distribution is to fit on the broad tails at higher angles. In aluminum, the angular correlation data can also easily be understood on the present theory although the total rate is overestimated by $\sim 25\%$ to be compared with no more than a few percent discrepancy in sodium.

ACKNOWLEDGMENTS

We have benefited from many clarifying discussions with Ed Woll, Jr. Interesting conversations with A. T. Stewart and S. Kahana are also gratefully acknowledged.

¹⁷ A. T. Stewart and J. B. Shand, *Phys. Rev. Letters* **16**, 261 (1966).

¹⁸ A. T. Stewart, J. B. Shand, and S. M. Kim., *Proc. Phys. Soc. (London)* **88**, 1001 (1966).

¹⁹ C. K. Majumdar, in *Proceedings of the Positron Annihilation Conference* (Academic Press Inc., New York, 1967); *Phys. Rev.* **149**, 406 (1966).

²⁰ D. R. Hamann, *Phys. Rev.* **146**, 277 (1966).

²¹ J. Crowell, V. E. Anderson, and R. H. Ritchie, *Phys. Rev.* **150**, 243 (1966).

²² D. J. W. Geldart and S. H. Vosko, *Can. J. Phys.* **43**, 1187 (1966).